The Effects of Superheat and Surface Roughness on Boiling Coefficients

H. M. KURIHARA and J. E. MYERS

Purdue University, West Lafayette, Indiana

The effects of liquid superheat and surface roughness on boiling coefficients were investigated in a series of experiments in which water, acetone, *n*-hexane, carbon tetrachloride, and carbon disulfide were boiled on a flat plate. In addition to the usual thermal measurements, the number of active boiling centers was determined, whenever possible, by visual means, and a quantitative measure of surface roughness was made. It was found that the number of active boiling centers on the plate increased with increasing surface roughness and that the calculated boiling coefficients were proportional to the one-third power of the number of bubble columns rising from the heated surface.

An equation has been derived relating boiling coefficients to fluid properties and the number of active boiling centers on a surface. A second equation, based on the theory of thermal fluctuations, has been proposed to relate the number of active boiling centers to the independent variables of surface-roughness and temperature-difference driving force. The limited data available have been found to follow this proposed relation.

The results of this work suggest a quantitative method of relating the boiling coefficient to the character of the surface which may explain the discrepancies observed in the slopes of boiling curves reported in the literature and in the actual values reported for the boiling coefficients measured on different surfaces.

When a liquid boils, vapor bubbles are formed and rise from favored spots on the heated surface. This type of boiling is called *nucleate boiling*, since it suggests the presence of some kind of nuclei at the points where the bubbles are formed. As the temperature of the surface increases, the number of active centers increases. However at high degrees of superheat the surface may produce vapor at such a rate that no active centers can be distinguished. Neither this condition, called *film boiling*, nor the transition zone between nucleate and film boiling was encountered in the present investigation.

It has been generally agreed (*13, 14, 15, 25, 27*) that the high heat transfer rates encountered in nucleate boiling are due primarily to the agitation created by the motion of the bubbles in the superheated liquid adjacent to the heater surface. Hence a knowledge of both bubble dynamics and the factors which determine the concentration of active centers would seem to be essential if the boiling process is to be understood and boiling performance predicted.

The development of a bubble has ben studied theoretically. On the basis of the work of Bashforth (*3*) and Wark (*28*), Fritz (*12*) obtained a semiempirical relationship for the diameter of a bubble breaking off the heating surface which showed good agreement with the experimental results of Jakob (*17*) and Kabanow and Frumukin (*18*). From a photographic study Jakob (*16*) discovered that the product of bubble diameter and the frequency of bubble formation seemed to be constant at small heat fluxes. More recently Perkins and Westwater (*23*) found that, at heat fluxes up to 80% of maximum, the individual terms of bubble diameter and frequency were constant themselves. From this they concluded that the increase in the boiling coefficient with increase in temperature-difference driving force was caused entirely by an increase in the number of active sites on the heating surface.

Early investigations of the effects of surface condition on boiling have been reported by Jakob and Fritz (*15*) and Sauer (*26*). A recent paper by Clark, Strenge, and Westwater (*7*) describes experiments in which pits and scratches in the metal surface were found to provide most of the nucleation sites. No nuclei appeared to be associated with grain boundaries. Nishikawa (*21*) photographed the formation of steam bubbles rising from horizontal heating surfaces fitted with concentric grooves of triangular cross section, their depths ranging from 0.1 to 0.3 mm. He observed a greater number of bubble columns on a rough surface than on a smooth one and found the boiling coefficients to be higher on the rough surface. A large effect of microroughness on the ΔT necessary to sustain nucleate boiling at a given heat flux was shown by Corty and Foust (*8*). They postulated a vapor-trapping mechanism to explain large differences in the slopes and positions of boiling-coefficient curves for surfaces of different roughness. Bankoff (*2*) has derived a theory to determine whether a surface cavity will entrap gas in contact with a liquid.

Attempts have been made by various investigators to obtain a better knowledge of the mechanism with the aid of nucleation theory. LaMer (*20*) and Bernath (*5*) reviewed the theory of Volmer (*27*) and Becker and Döring (*4*) as applied to the formation of vapor bubbles in liquids. Clark (*6*) has extended the kinetic theory of heterophase thermal fluctuations, given by Frenkel (*11*) for nucleus formation, and derived a relation between superheat required for nucleation and liquid properties.

Westwater (*29*) has summarized a number of empirical equations which have been prepared by correlating experimentally measured boiling coefficients. Recently semitheoretical equations proposed by Rohsenow (*24*) and Forster and Zuber (*9*) have met with some success in correlating results. Both equations contain modified Reynolds number groups as well as the conventional Prandtl number. The equation of Rohsenow is based on the observation of a constant product of frequency and bubble diameter as observed by Jakob (*16*). Forster and Zuber (*10*) have derived analytical expressions for bubble radii and growth, and these are employed in their proposed correlation referred to above. The main difference between the two equations is that in Rohsenow's equation the Reynolds number is based on the motion of the bubble when it is on the point of breaking off the heating surface, while in the Forster and Zuber equation the velocity in the Reynolds number term is taken as the rate of radial movement of the bubble wall.

None of the correlations referred to by Westwater contain terms which describe the nature of the heating surface, although many experimental investigations have shown that the condition of the heating surface has a major effect on boiling performance. The reason for this omission is due largely to the difficulty of describing a surface quantitatively. Until the time when the essential elements of a surface which affect boiling can be measured and are related mathematically to boiling performance, it is unlikely that any truly reliable correlation will be developed.

In the present investigation (*19*) the boiling surface was prepared before each run by polishing with emery paper to produce different degrees of roughness. The dimensions of the irregularities produced were then determined by use of a Brush surface analyzer, which recorded surface profiles. Thirty-four

H. M. Kurihara is with Shell Sekiyu Company, Ltd., Tokyo, Japan.

boiling runs were made with water, acetone, *n*-hexane, carbon tetrachloride, and carbon disulfide. The bubble columns rising from the heated surface were counted whenever possible. In addition heat flux and temperatures were measured so that boiling coefficients might be calculated. A mechanism to explain how surface roughness affects bubble formation has been postulated and a correlation found relating the number of active boiling centers to the distribution and size of the protuberances on a surface.

EXPERIMENTAL APPARATUS

The heater, shown in Figure 1, consisted of a copper cylinder 3 in. in diameter. Boiling took place on the upper surface of the cylinder, and the heat was supplied to seven copper fins (¼ in. thick and 2 in. high) which were welded to the bottom of the cylinder. The 1/5-in. spaces between the fins contained heating elements made by wrapping nichrome ribbon on a mica core. The elements were connected in series and had a total resistance of 15 ohms. A 5-in. O.D. stainless steel skirt (A.I.S.I. No. 301) was silver-soldered around the top of the copper cylinder to give a continuous nonboiling surface next to the surface on which boiling was taking place. The cylinder and skirt were then machined until the skirt was reduced to a thickness of 1/16 in. and the junction between copper and stainless steel was as free from irregularities as possible.

Figure 2 shows the location of the thermocouples. Three thermocouples were located ⅛ in. below the heating surface at various distances from the axis of the heater. Three others were placed ⅜ in. directly beneath the first three couples. Four thermocouples were fastened under the stainless steel skirt to determine its temperature gradient during operation.

Boiling took place in an 8-in.-diameter inverted glass bell jar 11 in. high. The jar was bolted to the top of the heater and sealed by a Teflon-jacketed sponge-rubber gasket as shown in Figure 3. An immersion heater consisting of a resistance wire inserted in a 6-mm. glass tube circled the periphery of the heater to help maintain a constant bulk liquid temperature over the heating surface during runs at low heat loads.

All the thermocouples employed were calibrated against a standard N.B.S. thermometer in an oil bath. Temperatures were recorded to 0.1°C. Power for the heater was obtained from a single-phase 220-v. a.c. source. Heat input was determined with two wattmeters to cover the range of 0 to 4,000 w. Voltage and current were checked with a 300-v. voltmeter and a 25-amp. ammeter.

Roughness of the heating surface was measured before and after each run by a Brush Surfindicator Model No. 110, which measures roughness by interpreting the motion of a diamond tip as it travels over a surface (*1,*). The instrument indicated a measure of the roughness in terms of the root-mean-square, but as a more accurate picture of the roughness of the surface was desired, a Brush Model BL-103 Surface Analyzer was also employed (*22*). This latter instrument consists of three parts: a motor-driven pick-up arm, a calibrating amplifier, and a direct-inking oscillograph. A spherical-tip diamond stylus with a tip radius of 0.0005 in. was attached to the crystal in the pick-up, which moved back and forth over the surface in a 10-sec. cycle. The voltage generated in the crystal by the vertical motion of the stylus was amplified, and it actuated the pen motor of the oscillograph so that a record of the surface irregularities encountered by the stylus was obtained on a moving-paper tape. The instrument was set to record in microinches and was calibrated by moving the stylus over a precision scratch on an attached glass standard.

EXPERIMENTAL PROCEDURES AND MEASUREMENTS

The heating surface was polished with six grades of emery paper (4-0, 3-0, 2-0, 0, 1, 2) and boiling measurements were taken for each surface roughness. One additional surface roughness was produced by polishing with 140-mesh carborundum. The emery paper was wrapped around a steel rod ½ in. in diameter and 3½ in. long, and the polishing was done systematically, by rubbing ten strokes in one direction and then ten strokes at an angle of 90 deg. to the initial direction. This procedure was repeated until the surface was considered thoroughly polished and reproducible.

Initially the roughness was measured before and after each run. Later it was found that the surface-roughness measurements did not change during runs with liquids other than water; measurements for these liquids were then made only before runs. Each surface-roughness determination was based on six readings, three being taken in each of the two directions in which the surface was polished.

The boiling vessel was operated with a liquid level just above the reflux return as shown in Figure 3. Because the system used a great deal of heat, it was usually necessary for vigorous boiling to be maintained for 2 hr. before the thermocouples in the system indicated that thermal equilibrium had been reached. When more than one set of measurements was taken during a single period of operation, they were always made by lowering the heat input. Condensate was returned to the system at temperatures as close to saturation as possible, and during operation at low heat loads the ring immersion heater was turned on to keep the bulk of the liquid at saturation temperature.

The measurements taken, in addition to surface-roughness readings, included the following:

1. Liquid bulk temperature was measured with a mercury thermometer placed at the center of the heater ½ in. above the heating surface.
2. Temperatures in the copper cylinder and stainless steel skirt were determined from thermocouples placed as shown in Figure 2.
3. Total heat input was determined from a wattmeter reading of the power supplied to the heater. The heat transfer rate normal to the boiling surface was determined by subtracting the rate of heat transfer through the skirt from the total heat input. The boiling-heat load was checked by condensate measurements and found to agree with a difference less than 5% for all but the lowest heat loads. Skirt losses, which were calculated from the temperatures determined by the thermocouples on the skirt, ranged from 2 to 25%.

During boiling, whenever possible, the

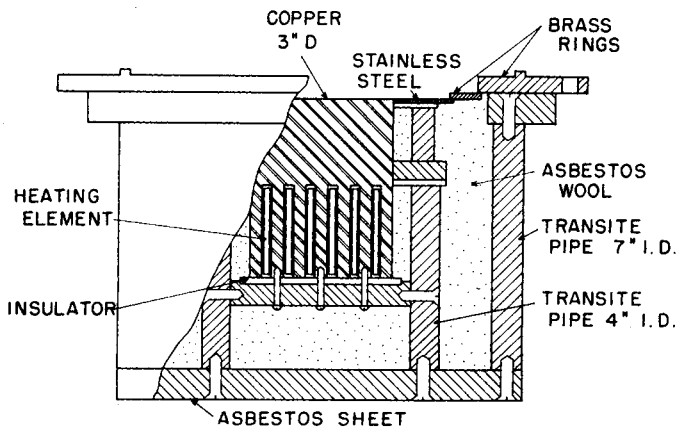

Fig. 1. Heater details.

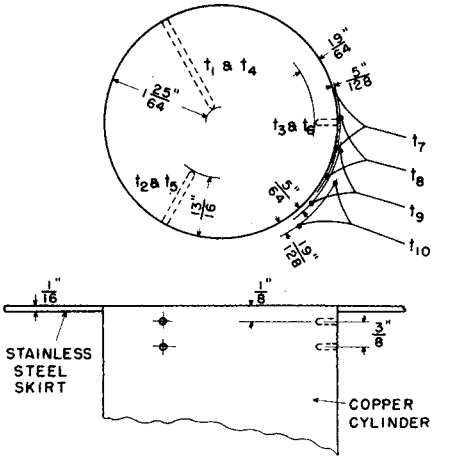

Fig. 2. Locations of thermocouples.

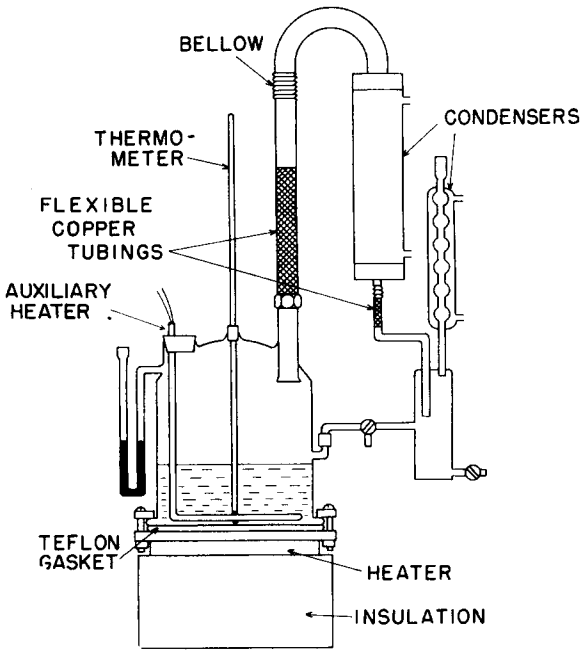

Fig. 3. Boiling apparatus for regular runs.

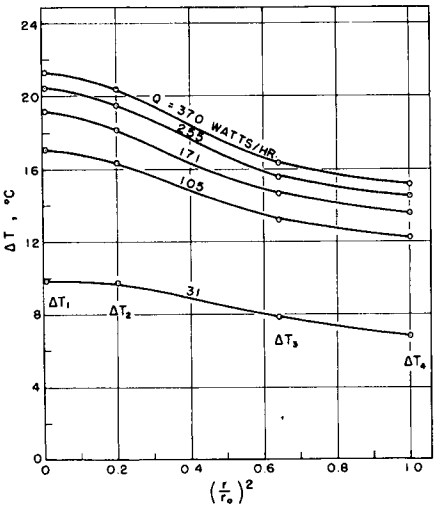

Fig. 4. Temperature difference driving force vs. $(r/r_o)^2$, run B-I-2.

active boiling sites on the heater surface were counted. Although, the experimental results contain bubble populations as high as 4,000/sq. ft., it should be kept in mind that this figure corresponds to only 196 centers on the 3-in.-diameter heating surface. This was found to be the upper limit at which visual counting could be done. Most of the data however were obtained in the range of 200 to 2,000 centers/sq. ft., which meant counting only ten to one-hundred centers on the heating surface. After a few runs, counting skill was developed, and it was found that in this range the counts were reproducible within 10%.

A sample of the experimental data is shown in Table 1. The temperatures from the respective thermocouples are located as follows:

Thermocouples located in copper cylinder

	Distance from wall, in.	Distance from surface, in.
t_1	1-25/64	1/2
t_2	13/16	1/2
t_3	19/64	1/2
t_4	1-25/64	1/8
t_5	13/16	1/8
t_6	19/64	1/8

Thermocouples attached to stainless steel skirt

	Distance from copper cylinder, in.
t_7	0
t_8	5/128
t_9	5/64
t_{10}	19/128

Surface temperatures on the cylinder, obtained by a linear extrapolation of the temperatures measured in the block, were considered to be accurate within ±0.2°C., and so the error in the resulting temperature-difference driving force was usually less than 2%. The temperature gradient in the skirt adjacent to the copper wall was used to determine the rate of heat dissipation through the skirt as mentioned above.

The heat transfer rate through a differential element of area may be written as

$$dq = h\,\Delta T\,dA \qquad (1)$$

which may be integrated and solved for q if the variation of h and ΔT are known over the surface. A mean heat transfer coefficient may be defined by the equation

$$q = h_m \int_o^A \Delta t\,dA \qquad (2)$$

and a mean driving force by the equation

$$q = h_m A\,(\Delta T)_m \qquad (3)$$

Equations (2) and (3) may be combined to show that

$$\Delta T_m = \frac{\int_o^A \Delta T\,dA}{A} = \int_o^1 \Delta T\,d(r/r_o)^2 \qquad (4)$$

Values of ΔT, calculated with the aid of the data in Table 1, were plotted against $(r/r_o)^2$ as shown in Figure 4. A graphical integration of each curve shown in Figure 4 provided the value of ΔT_m for each corresponding run. This was then used to obtain the mean boiling coefficient for each run as defined in Equation (3). The value used for q in Equation (3) was the electric heat load supplied to the heater minus the calculated skirt loss in each run.

The calculated values of the mean heat transfer coefficients are shown in Figures 5 to 9. The key for identifying the runs is as follows:

1. The alphabetical designations indicate the fluid used—*A*: water, *B*: acetone, *C*: *n*-hexane, *D*: carbon tetrachloride, *E*: carbon disulfide.

2. The Roman numerals indicate the types of polishing paper used in preparing the surface before boiling.

Roman numeral	I	II	III	IV	V	VI	VII
Emery paper	4-0	3-0	2-0	0	1	2	140-mesh carborundum

3. The Arabic numerals indicate different runs with one particular fluid and a single surface condition. For example run *B*-I-2 is the second run made with acetone boiling from a surface polished with 4-0 emery paper.

The qualitative effects of surface roughness are indicated on Figures 5 to 9. In each case the smoothest surface (obtained with 4-0 emery paper) gave the lowest boiling coefficients. Rougher surfaces gave not only higher boiling coefficients but boiling curves of larger slope, as was also observed by Corty and Foust (*8*). It also appeared that the effect of roughness on h_m became less pronounced as roughness increased. This implies a roughness limit above which boiling coefficients will not be affected by surface roughness. The order of magnitude of this limit is estimated to be 30 μin. (root-mean square).

A number of runs were reproduced with considerable success, as is shown in Figures 5 and 6. The duplicate runs were made after intervals of 24 hr. to check the possibility of aging of the surface.

During some runs at high heat loads, bubble columns were observed rising from the boundary between the heating surface and the skirt. However this number was estimated to be less than 1% of the number of columns issuing from the remainder of the boiling surface, and so they were neglected. At no time was boiling observed on the stainless steel skirt.

CORRELATION OF RESULTS

Although many equations have been derived relating boiling coefficients with physical properties, they have failed to indicate the effect produced by the surface condition of the heater. Since heat transfer to a boiling liquid seems strongly affected by surface roughness, it was decided to attempt a new correlation which would include both liquid and surface properties.

Heat flux (q/A) was plotted against

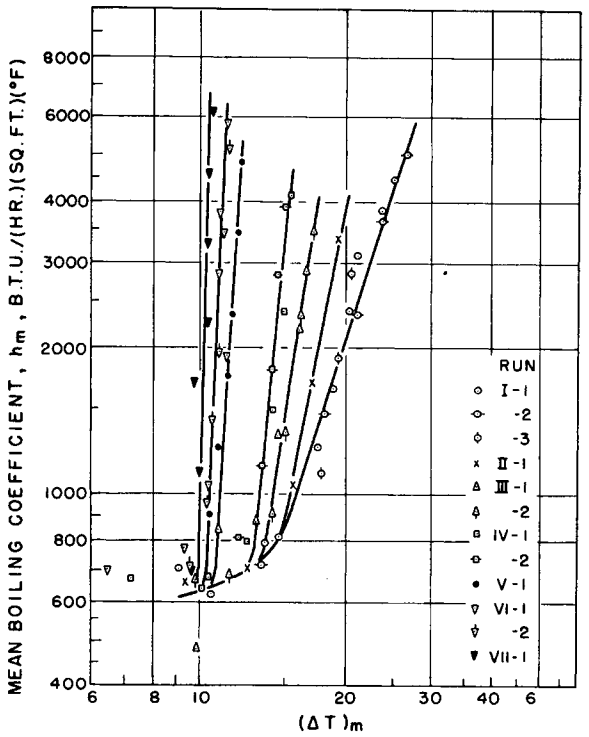

Fig. 5. Boiling curves for water.

the number of active centers, and it was seen that

1. q/A is not proportional to n as Jakob (16) observed but is rather proportional to n^m.
2. A rough surface gives a greater number of bubble columns than a smooth surface at a given heat flux.
3. The exponent m appears to be smaller for a rough surface than for a smooth surface.

As the next step, h_m was plotted against n with the result that h_m was found to be approximately proportional to $n^{1/3}$ for all liquids used and all surface conditions. The majority of the data were obtained for water and acetone; only these results are shown for the different surface conditions in Figure 10. The data at low values of h_m do not follow the above relationship, and it is felt that this may be due to the effect of the additional convection caused by the immersion heater. Although the bell jar was insulated, this heater was necessary to keep the bulk of the liquid at its saturation temperature at low heat loads. It was observed during operation that if this heater was cut off for a short period of time, a number of extra bubble columns appeared on the boiling surface to help dissipate the same heat load.

As the first step in the correlation an attempt was made to relate the boiling coefficient h_m to the number of bubble columns as well as to the physical properties of the liquid. Rohsenow (24) has defined

$$N_{Nu} = \frac{h_m D_b}{k_l}$$

$$N_{Re} = \frac{G_b D_b}{\mu_l}$$

$$N_{Pr} = \frac{C_l \mu_l}{k_l}$$

Combining these groups in the usual form of a dimensionless heat transfer equation gives

$$N_{Nu} = K' N_{Re}^{\ j} N_{Pr}^{\ w} \qquad (5)$$

When one assumes the bubbles to be spheres,

$$G_b = \frac{\pi}{6} D_b^3 \rho_o f n \qquad (6)$$

Substitution in Equation (5) gives

$$\frac{h_m D_b}{k_l} = K' \left(\frac{\pi D_b^4 \rho_o f n}{6\mu_l}\right)^j \left(\frac{C_l \mu_l}{k_l}\right)^w \qquad (7)$$

Introducing the relation $D_b f$=constant into the above equation and grouping all the constant terms together yields

$$\frac{h_m}{k_l} = K D_b^{3j-1} \left(\frac{\rho_o n}{\mu_l}\right)^j \left(\frac{C_l \mu_l}{k_l}\right)^w \qquad (8)$$

Since h_m was shown to be approximately proportional to $n^{1/3}$, the term $j = 1/3$; thus $3j - 1$ equals zero, and the term D_b drops out of Equation (8). Although the complete omission of D_b may be only approximately correct, the effect of D_b on h_m will likely be small. Forster and Zuber (9) have shown theoretically that small bubbles grow faster than large bubbles, and so their contribution to the agitation of the fluid is approximately the same.

Substituting $j = 1/3$ in Equation (8) gives

$$\frac{h_m}{k_l} = K n^{1/3} \left(\frac{\rho_o}{\mu_l}\right)^{1/3} \left(\frac{C_l \mu_l}{k_l}\right)^w \qquad (9)$$

A cross plot of $(h_m/k_l)(\mu_l/\rho_o)^{1/3}$ vs. Pr for a constant value of $n = 4{,}000$ was made, and the slope of the straight line was found to -0.89. Figure 11 shows a plot $(h_m/k_l)(\mu_l/\rho_o)^{1/3}(Pr)^{0.89}$ vs. n for all the runs (of all the fluids) in which the number of active centers was counted. The equation of the straight line in the graph is

$$\frac{h_m}{k_l} = 820 \left(\frac{\rho_o}{\mu_l}\right)^{1/3} n^{1/3} (Pr)^{-0.89} \qquad (10)$$

EFFECTS OF SURFACE ROUGHNESS

The next phase of the problem was to find a relationship between the number of active centers and the independent variables, ΔT and surface roughness. Thorough discussions of existing notions as to the sources of nuclei, given by Westwater (29) and Clark (6), may be summarized as follows:

1. Molecular groups are formed by thermal fluctuations of molecules with energies corresponding to the new phase.
2. Bubbles of sufficient size are formed by minute explosions of highly superheated liquid.
3. Nuclei are foreign particles or pockets of dissolved gas.
4. Nuclei consist of vapor or gas trapped in small crevices in a solid from which bubbles can form during boiling. In the present investigation all liquids were boiled for several hours before each run was started, and so the effect of dissolved gas was thought to be insignificant. According to Bankoff (2) the condition that a cavity or

Table 1. Sample Experimental Data*

Run B-I-2 (second run with acetone boiling on a 4-0 surface)

t_1	t_2	t_3	t_4	t_5	t_6	t_7	t_8	t_9	t_{10}	t_l	W, watts
79.6	79.2	76.2	78.0	77.2	73.4	71.8	67.8	64.0	63.0	56.2	370
75.9	75.6	72.9	75.5	74.7	71.4	70.0	66.6	63.3	62.4	56.2	175
66.0	65.9	64.1	66.0	65.9	64.0	63.0	61.7	60.2	60.1	56.2	31

* All temperatures in °C.

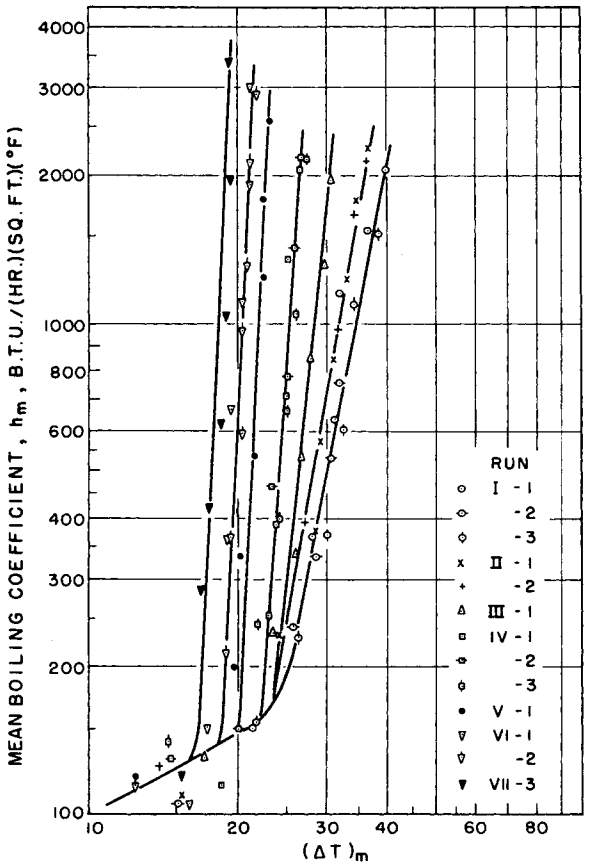

Fig. 6. Boiling curves for acetone.

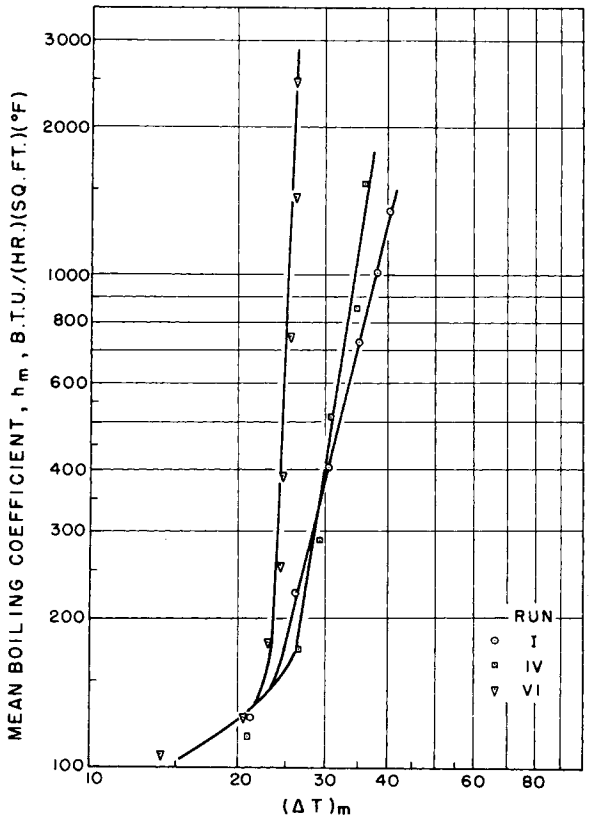

Fig. 8. Boiling curves for carbon tetrachloride.

groove entraps gas in contact with a given liquid is that $\theta > \phi$. Some of the roughness charts obtained in the present work were enlarged and analyzed for values of ϕ which were found to range from 160 to 170 deg. Since ϕ was of this magnitude, these grooves appeared to be very poor vapor traps; therefore condition 4 stated above did not appear to apply to surfaces of the type employed in the present study, although there is a definite possibility that the mechanism applies to certain

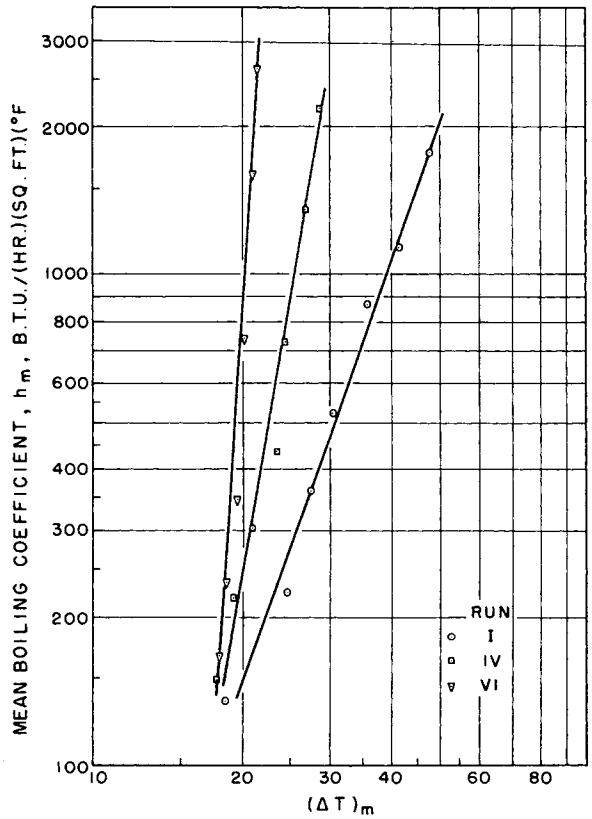

Fig. 7. Boiling curves for *n*-hexane.

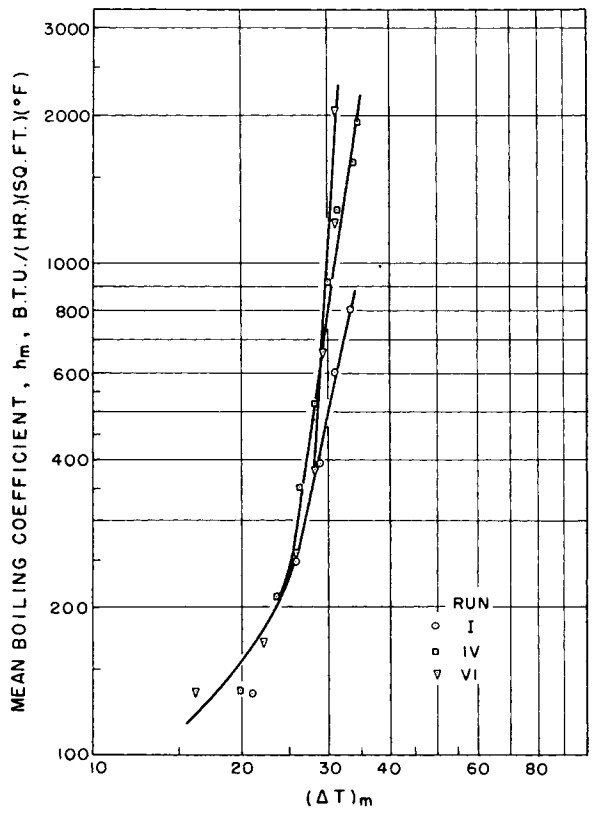

Fig. 9. Boiling curves for carbon disulfide.

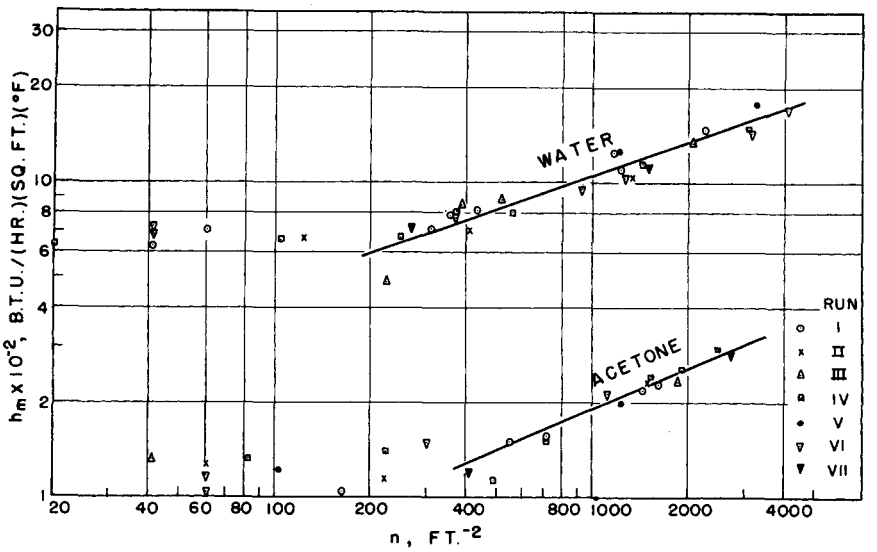

Fig. 10. Mean boiling coefficient vs. concentration of active centers for water and acetone.

surfaces. As not much seems to be known about condition 2, attention was turned to item 1.

The work required to form a nucleus having an apparent spherical radius has been given by Westwater (*30*) and Frenkel (*11*) as

$$\Delta Z = 4\pi\sigma(R^*)^2[(R/R^*)^2 - 2/3(R/R^*)^3] \quad (11)$$

where R^* is given by the equation

$$R^* = \frac{2\sigma}{p_g - p_l}$$

When $R = R^*$, Equation (11) becomes

$$\Delta Z^* = 4/3\,\pi\sigma(R^*)^2 \quad (13)$$

in which ΔZ^* may be considered an energy barrier which, if once surmounted, permits the autocatalytic process of vapor formation to proceed.

The problem is to find the number of nuclei of size R^* on a heating surface at a given degree of superheat. The Clausius-Clapeyron equation may be approximated in the form

$$\left(\frac{dp}{dT}\right)_o = \frac{\lambda}{v_g T} \quad (14)$$

Assuming that λ/v_g does not vary significantly, one may integrate Equation (14) to give

$$p_{o_2} - p_{o_1} = \frac{\lambda}{v_g} \ln\left(\frac{T_{o_2}}{T_{o_1}}\right) \quad (15)$$

If p_{o_1} is taken as p_l, T_{o_1} may be written as T_o. Then

$$p_{o_2} - p_l = \frac{\lambda}{v_g} \ln\left(1 + \frac{T_{o_2} - T_o}{T_o}\right) \quad (16)$$

If T_{o_2} is taken as the temperature inside the bubble at the instant of nucleation, it represents the superheat temperature. The pressure inside the bubble will be nearly equal to the vapor pressure at T_{o_2}. If $T_{o_2} - T_o$ is small compared with T_o, then equation (16) becomes

$$p_g - p_l = \frac{\lambda}{v_g}\frac{\Delta T}{T_o} \quad (17)$$

Combining Equations (12) and (17) gives

$$R^* = B/\Delta T \quad (18)$$

where

$$B = \frac{2\sigma v_g T_o}{\lambda} \quad (19)$$

Thus R^* is approximately inversely proportional to ΔT. However it should be noted that Equation (18) does not tell at what ΔT a liquid starts boiling but simply gives the size of the nucleus which is in a state of equilibrium at that degree of superheat. A nucleus smaller than this should dissipate itself, and one larger should grow.

As the experimental results of this investigation show, the shape, size, and size distribution of surface grooves have an essential influence on bubble formation during nucleate boiling. In his photographic study of boiling methanol Westwater (23) showed that the size of a bubble from an active center remains constant during nucleate boiling. This means that an active center, which may be a valley or groove of certain size, generates bubbles of a constant size regardless of the heat flux or ΔT when bubbles have once started to form from that spot. Thus the volume elements of superheated liquid in grooves having a radius of R^* may be the nuclei for the formation of bubbles of initial radius R^* at the corresponding ΔT. From this it follows that the number of nuclei of a certain size may be expected to be proportional to the number of grooves of corresponding size. However although there were numerous grooves of approximately the same size on a polished surface, as seen from the measured surface profiles, and all those of size R^* could have provided nuclei according to the above theory, the number of bubble columns observed was always far smaller than the number of suitable grooves. In other words, only a small fraction of the available sites were activated.

Since the process of nuclei formation requires an activation energy, one may assume, as suggested by Frenkel (*11*), that the number of nuclei of size R is distributed according to the Maxwell Boltzman expression:

$$P_R = C_1 \exp.\left(\frac{-\Delta Z}{m'R'T}\right) \quad (20)$$

This may be interpreted as follows. At a given degree of superheat, nuclei

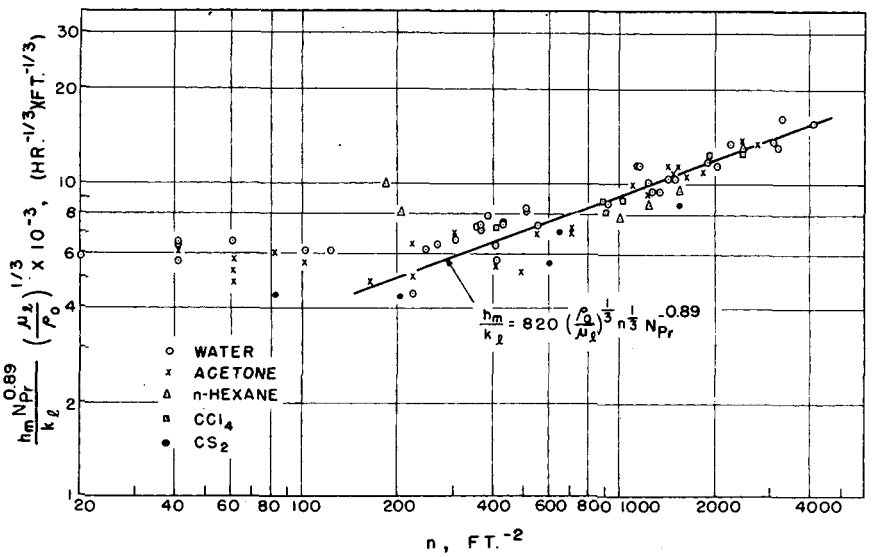

Fig. 11. Correlation of boiling coefficient with concentration of active centers.

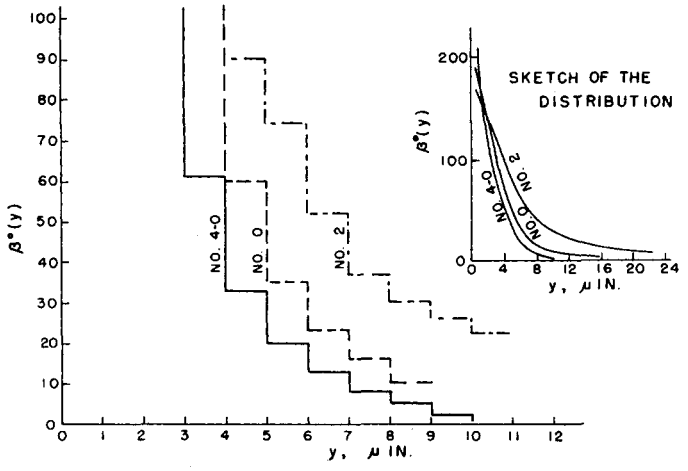

Fig. 12. Groove-size distribution on heating surfaces.

are constantly forming and dispersing owing to heterophase fluctuations, and the distribution follows the Boltzman expression. At a given ΔT all nuclei having radii smaller than R^* cannot grow, but disperse immediately.

If $\beta(R)$ represents the number of grooves of size between R and $R+1$ units over a unit area of heating surface, and β_t the total number of grooves of size between R_o and R, then the change from R to $R + dR$ will be accompanied by a change in β_t of $\beta(R)\,dR$. Therefore

$$d\beta_t = \beta(R)dR \qquad (21)$$

and the change in the number of active nuclei accompanied by a change of R may be expressed as

$$dn = P_R\,\beta(R)dR \qquad (22)$$

From Equation (18)

$$dR = \frac{-R}{\Delta T}d(\Delta T) = \frac{-R^2}{B}d(\Delta T) \qquad (23)$$

The superscript * is no longer necessary, since any R is potentially the critical radius at its corresponding ΔT.

Substituting Equation (23) in Equation (22) and integrating from ΔT_1 to ΔT_2, one gets

$$n_2 - n_1 = \frac{-1}{B}\int_{\Delta T_1}^{\Delta T_2} P_R R^2 \beta(R)d(\Delta T) \qquad (24)$$

Furthermore from Equations (13) and (20)

$$P_R = C_1 \exp\,(-4\pi\sigma R^2/3\,m'R'T_o) \qquad (25)$$

If one postulates the existence of a cone in a groove with depth y, one finds that

$$m' = 1/3\,(R^2\pi y\,\rho_l) \qquad (26)$$

Combining Equations (24), (25), and (26) and using the relation $R = y \tan(\phi/2)$, one gets

$$n_2 - n_1 = -\frac{C_1}{B}\int_{\Delta T_1}^{\Delta T_2} R^2\,\beta(R)\exp\left(\frac{-E}{R}\right)d(\Delta T) \qquad (27)$$

where

$$E = \frac{4\sigma\tan(\phi/2)}{\rho_l R'T_o} \qquad (28)$$

As may be seen, Equation (27) contains the constant C_1 and hence cannot be used to predict n at a given ΔT for the liquid under consideration. However the applicability of the equation may be shown by the following method.

First $\beta(R)$ must be obtained. Because of the difficulty of measuring the values of R from the strip charts, the groove depths were determined instead, and their distribution was assumed to be the same as $\beta(R)$. As described earlier, ϕ was found to be approximately constant for all grades of emery paper used, and so, although the depth of the valleys varied greatly, their shapes were similar.

Figure 12 shows $\beta^\circ(y)$ vs. y for surfaces polished with numbers 4-0, 1-0, and 2 emery paper. $\beta^\circ(y)$ is the average of the six sets of surface measurements taken on each surface at the locations indicated earlier. $\beta(y)$ was assumed to be related to $\beta^\circ(y)$ by the equation

$$\beta(y) = C_2\,\beta^\circ(y) \qquad (29)$$

where C_2 is characteristic of the roughness. Equation (27) becomes

$$n_2 - n_1 = \frac{C_3}{B}\int_{\Delta T_1}^{\Delta T_2} R^2\,\beta^\circ(y)\exp\left(\frac{-E}{R}\right)d(\Delta T) \qquad (30)$$

where $C_3 = -C_1C_2$. The values of B and E were calculated for each liquid and are shown in Table 2. The right-hand side of Equation (30) was then integrated graphically between two values of ΔT_1 and ΔT_2, so that C_3 might be determined for one liquid for each kind of surface. For the 4-0 surface C_3 was found to be 4.1 from data taken with acetone. For the 1-0 surface $C_3 = 3.5$ from acetone data and for the No. 2 surface $C_3 = 3.3$ from carbon disulfide data. With the experimental value of C_3 for each surface and one experimental set of readings of the number of nuclei at a certain degree of superheat (ΔT_1), the number of active nuclei could be calculated at other ΔT's. This was done for the three surfaces in question, and the results are shown in Figures 13, 14, and 15 compared with the experimental data. Tables 2 and 3 show the constants

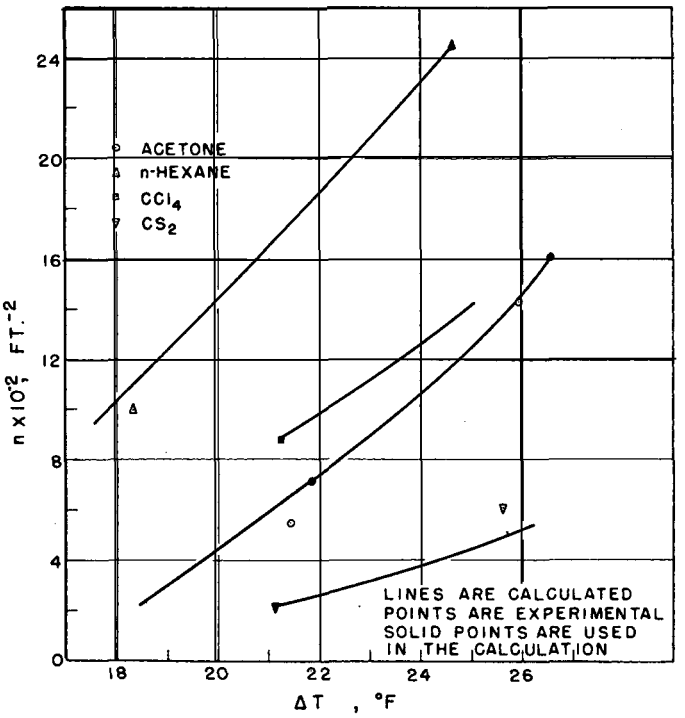

Fig. 13. Comparison of concentration of active centers calculated by Equation (30) with experimental data for number 4-0 polished surface.

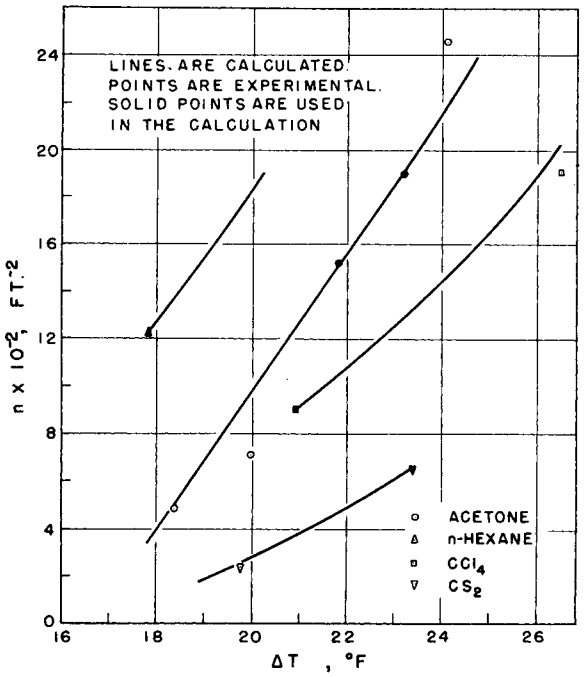

Fig. 14. Comparison of concentration of active centers calculated by Equation (30) with experimental data for number 1-0 polished surface.

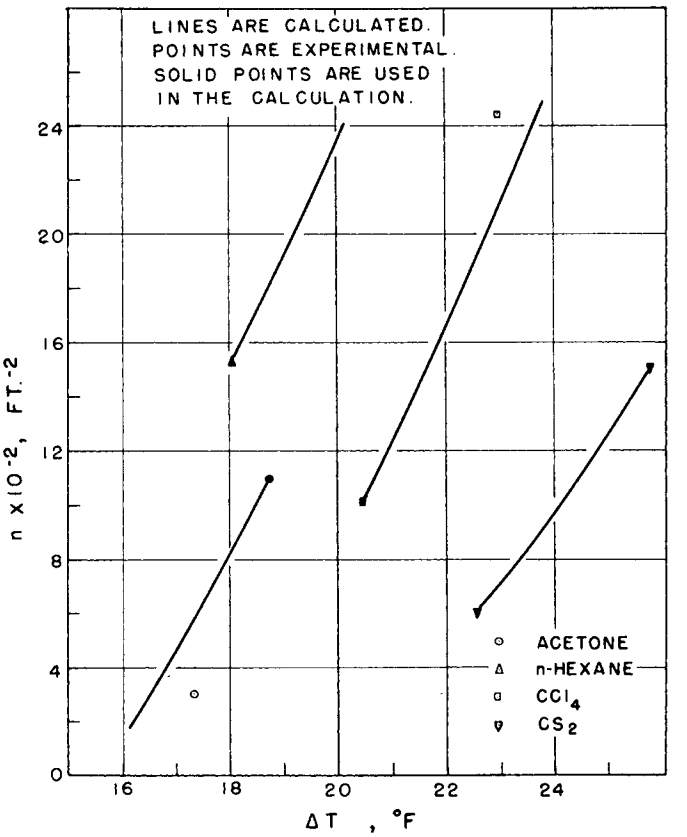

Fig. 15. Comparison of concentration of active centers calculated by Equation (30) with experimental data for number 2 polished surface.

used in the integration indicated in Equation (30) and a sample of some of the data and results.

Unfortunately not many values of n were available to test the validity of Equation (30), because the number of active centers increased so rapidly with heat flux that it was impossible to count them by eye above a certain limit. Furthermore the data at low heat fluxes could not be used because of the natural-convection effects of the immersion heater which were mentioned earlier. However the data available seem to behave as predicted by Equation (30), which shows the extremely sensitive effect of groove-size distribution on the number of active centers.

Calculations were not made for water for the following reason. The value of the term B for water is extremely large [2,300 (μin.)(°R.)] compared with that for other liquids (600 to 1,300). The radius of a nucleus computed from the value of B is about 150 μin. This corresponds to a valley depth of 20 μin. or more. Although there is almost no valley of that depth on a surface polished with 4-0 emery paper, many activated spots were observed during runs on this type of surface. This may be due to the possibility that, when the critical radius of a nucleus is very large compared with the available groove size, the nucleus could possibly be formed over several grooves. In this case $\beta(R)$ could not be predicted, since it is not indicated by a simple $\beta°(y)$ for the surface. This tendency may exist for a nucleus of any size but will not be significant for small nuclei.

The proposed mechanism has several uncertain points. Contact angle was not taken into account because even if it were available for macroscopic systerms it might not be the same on a microscopic scale. Furthermore C_1 was assumed to be constant as suggested by Frenkel (*11*). However it is actually a function of temperature and thus may have varied to some extent.

Since the effect of groove-size distribution is so important, it is essential to obtain a surface profile which represents the surface exactly. The surface analyzer is an excellent instrument to measure surface roughness. Even so it is questionable whether one can extend a surface profile taken in a linear direction to represent the area under consideration. Although the valleys were assumed to be cone shaped, actually they probably had more complicated profiles.

A further difficulty arose from the use of ΔT_m for ΔT in the calculation of n in Equation (30). During boiling the temperature of the center of the heater was greater than near the wall. As a result a greater concentration of bubble columns existed near the center of the heating surface. To carry out the calculations more precisely n should have been counted over concentric segments of the heater surface, where the temperature was more nearly constant. However this was impractical with the techniques used in this investigation.

Table 2. Values of B and E in Equation (30)

	Water	Acetone	n-hexane	CCl_4	CS_2
B(μin.)(°R.)	2330	790	620	960	1280
E(μin.)*	3.8	5.7	7.3	7.8	8.1

* Average groove bottom angle taken as 164 deg.

Table 3. Data for Correlation of Number of Active Centers, Acetone, 4-0 Polished Surface

ΔT, °F.	R, μin.	y, μin.	$e^{-B/R}$	$\beta°(y)$	Δn, ft.$^{-2}$	n, ft.$^{-2}$
26.5	30	4	0.83	61	470	1610
24.5	32	5	0.84	33	295	1140
22.5	35	5	0.85	33	357	845
20.5	39	6	0.86	20	270	488
18.5	—	—	—	—	—	218

CONCLUSIONS

Equation (10), relating the number of active centers to the boiling coefficient and Equation (30), relating the temperature-difference driving force to the number of active centers, offer a method of predicting the curve of h vs. ΔT for various liquids and surfaces. As

yet, some experimental information is necessary for the determination of certain constants, and in addition a graphical integration is necessary for the solution of these equations. However the equations have the present value of offering a quantitative interpretation of contradictory results in the literature, some of which are certainly due to surface effects. For example the equations make it apparent that for surfaces which have been highly polished and thus may have a very narrow spectrum of surface irregularities, the number of active boiling centers will be quite sensitive to changes in ΔT in the nucleate boiling zone. This would result in a high value for the slope of the curve of h vs. ΔT. The limiting situation would be a surface covered with cavities of identical size for which the equations would predict an infinite slope of the curve of h vs. ΔT.

ACKNOWLEDGMENT

Funds for this research were provided by the Purdue Research Foundation in the form of an X-R grant.

NOTATION

A = area of heating surface, sq. ft.

B = constant based on liquid properties, (μin.) (°R.)

C_l = specific heat of saturated liquid, B.t.u./(lb.-mass)(°F.)

C_1, C_2, C_3 = dimensionless constants

D_b = diameter of bubble when breaking off heating surface, ft.

E = characteristic term defined by Equation (28), μin.

f = frequency of bubble formation, sec.$^{-1}$

G_b = bubble flow rate, lb.-mass/(sq. ft.)(hr.)

g = acceleration of gravity, ft./hr.^{2}

g_c = conversion factor, 4.17×10^8 (lb.-mass) (ft.)/(lb.-force) (hr.^{2})

h = boiling coefficient, B.t.u./(hr.)(sq. ft.)(°F.)

h_m = mean boiling coefficient, B.t.u./(hr.)(sq. ft.)(°F.)

j = constant, dimensionless

K' = constant, dimensionless

k = thermal conductivity of saturated liquid, B.t.u./(hr.)(ft.)(°F.)

m = constant, dimensionless

m' = mass of liquid associated with one nucleus of radius R, lb.-mass

n = concentration of active centers, ft.$^{-2}$

Δn = difference between concentration of active centers at two different degrees of superheat, $n_2 - n_1$, ft.$^{-2}$

p_o = vapor pressure of saturated liquid, lb.-force/sq. ft.

p_g = pressure on vapor side of interface, lb.-force/sq. ft.

p_l = pressure on liquid side of interface, lb. force/sq. ft.

P_R = fraction of active nuclei of size R with respect to total number of nuclei, dimensionless

q = net heat input, B.t.u./hr.

R = radius of nucleus, μin.

R' = gas constant, (lb.-force)(ft.)/(°R.)(lb.-mass)

R^* = critical radius of nucleus, μin.

r = radial distance from the center of the heater, ft.

r_o = radius of copper cylinder, ft.

T_s = temperature at the surface of the heater, °C.

T_o = saturation temperature of liquid, °F.

t_l = temperature of boiling liquid, °C.

t_1, t_2, etc. = temperatures from the thermocouple readings, °C.

ΔT = temperature difference driving force, °C. or °F.

$(\Delta T)_m$ = mean temperature-difference driving force, °F.

v_g = specific volume of saturated vapor, cu.ft./lb.-mass

w = constant, dimensionless

y = depth of groove, μin.

ΔZ = free-energy change during fluctuation process, B.t.u.

ΔZ^* = nucleating free energy, B.t.u.

Greek Letters

$\beta(R)$ = number of grooves of size between R and $(R+1)$ units over unit area, ft.$^{-2}$

β_t = total number of grooves of size between R_o and R

$\beta(y)$ = number of grooves of depth between y and $(y+1)$ units over unit area, ft.$^{-2}$

$\beta^\circ(y)$ = number of grooves of depth between y and $(y+1)$ units over a distance of 1/16 in.

λ = latent heat of vaporization, B.t.u./lb.-mass

μ_l = viscosity of saturated liquid, lb.-mass/(ft.)(hr.)

ρ_l = density of saturated liquid, lb.-mass/cu. ft.

ρ_o = density of saturated vapor, lb.-mass/cu. ft.

σ = surface tension of vapor-liquid interface, dynes/cm.

ϕ = angle at the bottom of cone-shaped groove, radians

θ = bubble-contact angle, radians

Dimensionless Groups

N_{Nu} = Nusselt number

N_{Pr} = Prandtl number

N_{Re} = Reynolds number

Subscripts

o = saturation state

Superscripts

o = measurement of number of grooves; distinguishes them as being taken on a path 1/16 in. long

LITERATURE CITED

1. Albott, E. J., and S. Bousky, *Mech. Eng.*, **60**, 521 (1938).
2. Bankoff, S. G., *A.I.Ch.E. Journal*, **4**, 24 (1958).
3. Bashforth, F., "Capillary Action," Cambridge Univ. Press, London, England (1883).
4. Becker, R., and W. Döring, *Ann. Physik*, **24**, 719 (1935).
5. Bernath, L., *Ind. Eng. Chem.*, **44**, 1310 (1952).
6. Clark, J. A., *Mass. Inst. Technol. Tech. Rept. No. 7* (1956).
7. Clark, H. B., P. S. Strenge, and J. W. Westwater, *Chem. Eng. Progr. Symposium Ser. No. 29*, **55** (1959).
8. Corty, Claude, and A. S. Foust, *ibid.*, No. 17, **51** (1955).
9. Forster, H. K., and N. Zuber, *A.I.Ch.E. Journal*, **1**, No. 4, 531 (1955).
10. ———, *J. App. Physics*, **25**, 475 (1954).
11. Frenkel, J., "Kinetic Theory of Liquids," Oxford Press (1946); Dover Publications, New York (1955).
12. Fritz, W., *Phys. Z.*, **36**, 379 (1935).
13. Gunther, F. C., and F. Kreith, Heat Transfer and Fluid Mech. Inst., Berkeley, California (1949).
14. ———, *Calif. Inst. Technol. Progr. Rept.*, **44** (March, 1950).
15. Jakob, Max, and W. Fritz, *Forsch. Geb. Ing.*, **22**, 435 (1931).
16. Jakob, Max, "Temperature, Its Measurement and Control in Science and Industry," Reinhold, New York (1941).
17. ———, "Heat Transfer," p. 614, John Wiley, New York (1949).
18. Kabanow, B., and A. Frumukin, *Z. Phys. Chem.*, **165**, 433 (1933).
19. Kurihara, H. M., Ph.D. thesis, Purdue University, Lafayette, Indiana (1956).
20. La Mer, V. K., *Ind. Eng. Chem.*, **44**, 1270 (1952).
21. Nishikawa, K., *Trans. Soc. Mech. Engrs. (Japan)*, **20**, 808 (1954).
22. Operating Information of Brush Model BL-103 Surface Analyzer, Brush Electronics Co., Cleveland, Ohio.
23. Perkins, A. S., and J. W. Westwater, *A.I.Ch.E. Journal*, **2**, 471 (1956).
24. Rohsenow, W. M., *Trans. Am. Soc. Mech. Engrs.*, **74**, 969 (1952).
25. ———, and J. A. Clark, *ibid.*, **73**, 609 (1951).
26. Sauer, E. T., *et al., Mech. Eng.*, **60**, 669 (1938).
27. Volmer, M., "Kinetik der Phasebildung," Edward Brothers, Ann Arbor, Michigan (1945).
28. Wark, I. W., *J. Phys. Chem.*, **37**, 623 (1933).
29. Westwater, J. W., "Advances in Chemical Engineering," Vol. I., Chap. I, Academic Press, New York (1956).

Manuscript received November 12, 1958; revision received July 7, 1959; paper accepted July 10, 1959. Paper presented at A.I.Ch.E. Atlantic City meeting.